Extraction of Modal Parameters From Spacecraft Flight Data

George H. James, Timothy T. Cao, Vincent A. Fogt, Robert L. Wilson
Loads and Structural Dynamics Branch
NASA Johnson Space Center
Houston, Texas 77058

Theodore J. Bartkowicz
The Boeing Company
Space Exploration Division
Houston, Texas 77059

ABSTRACT
The modeled response of spacecraft systems must be validated using flight data as ground tests cannot adequately represent the flight. Tools from the field of operational modal analysis would typically be brought to bear on such structures. However, spacecraft systems have several complicated issues:

1. High amplitudes of loads;
2. Compressive loads on the vehicle in flight;
3. Lack of generous time-synchronized flight data;
4. Changing properties during the flight; and
5. Major vehicle changes due to staging.

A particularly vexing parameter to extract is modal damping. Damping estimation has become a more critical issue as new mass-driven vehicle designs seek to use the highest damping value possible. The paper will focus on recent efforts to utilize spacecraft flight data to extract system parameters, with a special interest on modal damping. This work utilizes the analysis of correlation functions derived from a sliding window technique applied to the time record. Four different case studies are reported in the sequence that drove the authors' understanding. The insights derived from these four exercises are preliminary conclusions for the general state-of-the-art, but may be of specific utility to similar problems approached with similar tools.

INTRODUCTION
The spacecraft launch environment is a highly complex event that is characterized by high amplitude input forces, highly variable loads, a wide spectrum of responses, constantly changing vehicle mass, active control interactions, and staging. At the same time, structural response analyses and loads estimations must be performed with models that are only partially validated using ground test data. In fact in modern design cycles, the access to diagnostic and environmental ground tests is also limited. To compound matters, project managers tend to reduce uncertainty factors designed to protect for loads increases and model unknowns. As a result, the designs progress rapidly before loads and structural problems are uncovered. This means that there are very few tools available to recover from structural dynamics issues in such a highly dynamic environment without costly redesigns late in the design cycle or in early operations.

One tool is the further reduction of any uncertainty factors that cover model unknowns, which are driven strongly by the need to know the modal frequencies. Since the ability to obtain good modal frequency information is limited by ground test availability, the flight data from early test flights and early operational flights must be used to estimate frequency values. Another of the tools available is to adjust the assumed damping values for the flight environment. Most structural dynamics specialists realize that damping is not a parameter that can be determined with any certainty (even in high controlled laboratory situations). However, vigorous discussions about damping in the flight environment are becoming a more common occurrence. The industry as a whole is very limited on tools and techniques to estimate damping from flight data. This paper contains information about early attempts to understand and develop frequency and damping estimation in the flight environment.

The obvious starting point for estimating modal parameters from a structure in the field is the current technology of Operational Modal Analysis (OMA) [1]. This rapidly advancing field of study is developing and applying techniques to es-

timate modal parameters for operational structures with response measurements but without a measure of the input forces. These techniques are focused on ground-based structures that are stable and long measurement times are generally available. There were attempts at operational modal analyses as early as the 1960's. However, it was in the 1990's before the early generalized techniques were available [2, 3]. There are two general classes of algorithms for performing OMA: (1) time history-based techniques that are generally related to Stochastic Subspace Identification (SSI) [1-6] and frequency domain-based techniques that are related to Frequency Domain Decomposition (FDD) [1, 4, 5, 6].

The technical basis for the early time domain approaches involved converting measured responses into auto and cross-correlation functions and processing with standard time domain modal analysis routines [3]. However, the more general SSI techniques directly integrate the correlation calculations and modal processing algorithms into a single step rooted in discrete time system identification theory [4, 6]. The earliest manifestations of FDD were peak picking and half-power bandwidth estimation schemes operating on the Power Spectral Density (PSD) functions [5]. However the advanced FDD algorithms refine the modal parameter estimates using powerful tools like the Singular Value Decomposition (SVD) [1, 5]. An interesting direction for frequency domain approaches involves the use of Hilbert transforms applied to PSD's to obtain biased Frequency Response Function (FRF) estimates [1, 7]. There is another direction in operational testing that is offering some hope for more fully understanding system dynamics is to estimate the forces acting on the system. This would allow more traditional FRF-based approaches to be used for system identification. These forces can be estimated via known mass changes to the system [8] or via hybrid analytical/experimental data [9].

There have been a limited number of reported attempts to analyze flight data to extract modal parameter information, although there are certainly many other unreported attempts. The time domain approaches based on correlation and SSI are generally used for flight data analyses as the rapidly changing vehicle properties do not allow the full advantages of the frequency-domain approaches to be realized. The responses are generally broken into a series of sliding windows, each of short duration, which are processed individually. If the loading and system characteristics are fairly constant over each window, then estimates of the changing parameters can be obtained as a function of flight time [10-17].

This paper will include four "case studies" with different levels of complexity to exercise these techniques. A lander case study is provided first, which provides some early insight with less complexity to cover the issues. The second case study is a pointer to a launch system analysis that has shown some of the same unusual features that the first case study contained but contains all of the complexities expected in a launch system. The third case study is a series of very simple analytical studies using single degree-of-freedom systems to gain insight into the most basic aspects of operational flight data analysis seen in the earlier exercises. The final case study is the analysis of a very rapidly changing system during an abort test, which is the most difficult launch system that one can envision. The insights gained from the observations of the earlier case studies has driven the approach to this very difficult data analysis. The end result of this work are preliminary conclusions for further advancement of the field of operational analysis of rapidly changing systems and specific application recommendations for similar problems.

TECHNICAL BACKGROUND

The procedure used in this work will be to calculate auto and cross-correlation functions from response data obtained from the vehicle under launch conditions. It has been shown that these correlation functions are composed of decaying sinusoids with the appropriate modal frequency and modal damping. These modal parameters are then extracted from the correlation functions using time domain extraction algorithms [3]. Since the vehicle and the launch environment are rapidly changing systems, a sliding window approach is used to repetitively analyze short segments of data and collect the information to track changing frequency and damping [10-13]. This utilizes automated environment for the time domain modal parameter extraction using a technique (called AUTO-ID) [18, 19]. The addition of this technique eases the computational burden of extracting parameters in a consistent manner from the multitude of correlation functions calculated from the sliding window segments of the random time histories to allow a rapid assessment of the data. It is expected that in-depth data analysis will follow using a combination of digital filtering [10, 11], time-zooming [17], or advanced SSI techniques [15].

CASE STUDY 1 – LANDER SYSTEM FLIGHT

The RR1 vehicle is a lander test craft built by Armadillo Aerospace. It was flown in a tethered hover flight for over 30 seconds to produce the data set used herein (see Figure 1). The RR1 flight data was unique in the respect that it was real flight data with high amplitude excitation, an active control system, and mass changes due to fuel use. However, this data set did not contain significant changes in natural environments or forward velocity effects as it was a hover test. The RR1 data set consisted of 31,000 samples of three low frequency accelerometers that were sampled at 1,000 samples per second and useful for 1.4 to 350 Hz (see Figure 2). The channels were ranged for +/- 16g with a .007g resolution.

Figure 1. RR1 Vehicle in Static and Tethered Flight Configurations

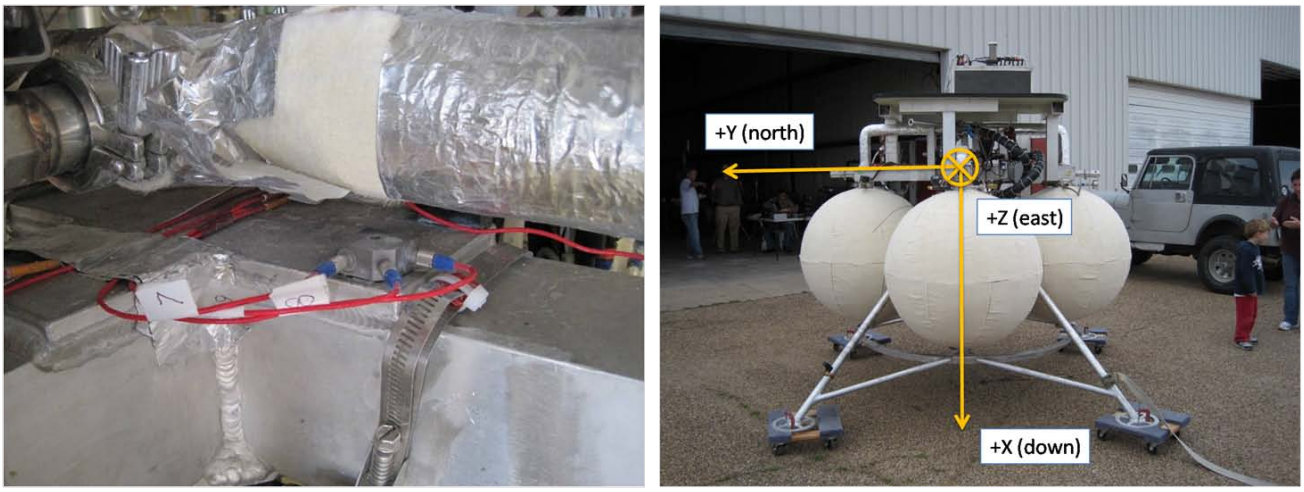

Figure 2. RR1 Vehicle Accelerometers and Coordinate System

The first use of the data was to assess the stability of the modal properties using a sliding window analysis with 2,000 point (2 sec.) windows. A 50% overlap or one thousand points (1 sec.) were skipped for each sliding window move. This allowed 30 different windows to be generated out of the full 31,000 sample time records. Nine cross and autocorrelation functions were calculated from the three sensors. AUTO-ID with the Eigensystem Realization Algorithm (ERA) was used as the modal engine [19]. The Consistent Mode Indicator (CMI) [20] was used with a 50% cut-off. Frequencies with damping values outside of 0% to 20% were excluded. Figure 3 shows the original data from the three sensors and the frequencies determined for each of the 30 different sliding windows. The data plots in Figure 3 show a strong Z direction mode near 30 Hz. Additional dynamic content is seen between 125 and 225 Hz with some content above 225 Hz (Y direction). The sliding window analysis shown in Figure 3 mirrors these observations. An important point is that neither the sensor magnitudes nor the extracted frequencies appear to change over the times selected.

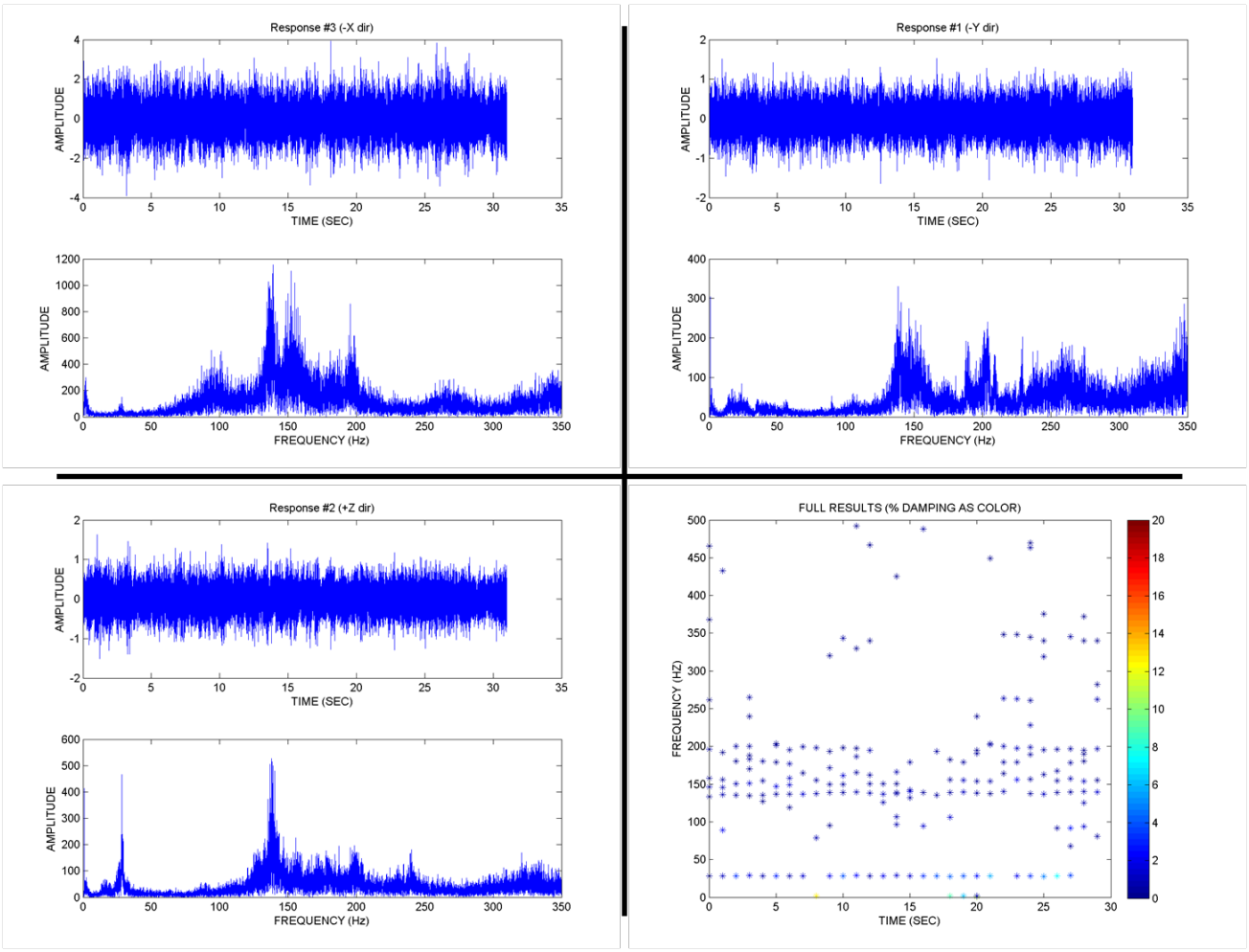

Figure 3. Three Axis RR1 Data and Sliding Window Analysis Results Using 30 Two Second Windows

Figure 4 shows the variations in frequency and damping for modes near 30, 130, 150, and 200 Hz. In the Figure 4 data near 30 Hz, reasonable stability in the frequencies and typical variations in damping is observed. The Figure 4 mode near 130 Hz plot, also shows reasonable stability in damping and frequency. In fact the frequency does show a minor increasing trend and the damping is more stable than the mode near 30 Hz. The modes near 150 and 200 Hz show the unusual characteristics of having stable damping but more variability in frequency. The important information here is that (in spite of the 130 Hz frequency) there is little apparent change in modal parameters over flight time.

The next logical step in the analysis of this data is to filter in around a frequency and use a limited dataset to more completely define specific frequency and damping. For this exercise, the Y direction sensor was used to attempt to refine the assessment of the mode near 30 Hz. A 4th order Butterworth forward/reverse 10-45 Hz bandpass filter was applied to the data. Figure 5 provides the resulting autocorrelation function (and autospectrum) as well as the frequency/damping results of processing each 1,000 lag window of the correlation function. It is important to note that the correlation function contains an unexpected "beating" after an initial decay, which manifests itself as instability in the frequency domain.

The correlation function in Figure 5 shows that the first part (approximately 2 seconds) of the trace looks like the expected decaying sinusoid, although the rest is dominated by the "beating". Table 1 shows the results of a more detailed assessment of the first 1,000 lags (one second). Analyses of the first, second, third, and fourth 250 lags are provided as well as an analysis of the first 1,000 lags (which envelopes all of the four 250 lag sets). It can be seen that a fairly consistent 28.2 to 28.3 Hz mode is seen. The short segment analyses have damping values that vary between 0.4% and 1.1%

with the full 1,000 lag analysis suggesting a damping value of 0.8%. It should be noted that the 1,000 lag analysis is the first data point on sliding window 1,000 lag analysis plots of Figure 5. Hence Figure 5 can be used to understand how the analysis results vary for subsequent 1,000 lag analyses. Table 1 also shows that there are additional higher damped loads in the early half second of the correlation functions. Therefore this data suggests that the first part of the correlation functions decay as expected and contain higher damped modes – but this is not conclusive. Additional insights will be gained using the numerical studies that will be discussed in an upcoming section.

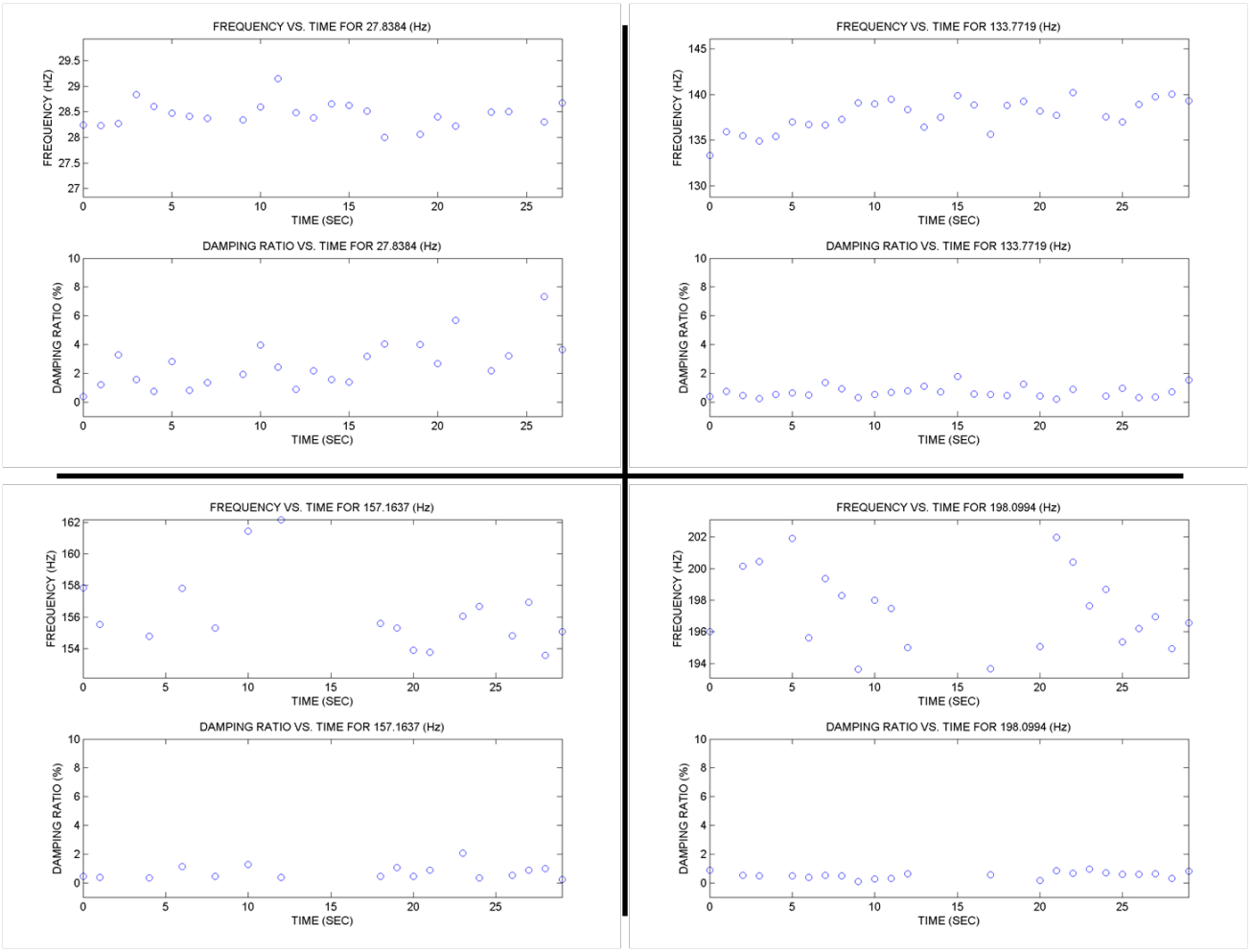

Figure 4. RR1 Frequency and Damping Sliding Window Variations for Modes near 30, 130, 150, and 200 Hz

CASE STUDY 2 – LAUNCH SYSTEM FLIGHT

The Ares1-X vehicle was a full-up launch system that flew first stage flight including motor ignition, liftoff acoustics, aerodynamic flight including maximum dynamic pressure, and motor burn-out. This flight data has a full suite of the characteristics seen in flight data and thus presents a more difficult analysis than the lander data in case study 1 above. The fifth author has performed a detailed independent analysis of this launch data and the reader is referred to reference [17] for details. As detailed in [17], the analyst identified the same problems with respect to unexpected "beating" at the higher time lags in the correlation functions.

CASE STUDY 3 – SIMPLIFIED NUMERICAL STUDY

The recent experience (discussed in previous sections) with the analysis of flight data has prompted the need to answer some basic questions concerning the data content and processing requirements. A simplified numerical study was performed to address the two most pressing issues seen in the case studies mentioned above: how does amplitude dependent

damping manifest itself in the analysis, and what is the source/mitigation of the beating phenomena. A single degree-of-freedom system was developed with a known frequency (10 Hz) and known damping values. Constant damping (2%) and amplitude-dependent damping were both modeled. Both impulse response and random excitations were applied to the system. Additive random noise of 0%, 5%, and 10% of maximum input force was added to the constant damping cases as a side study. The variable damping schedule for the impulse excitations was 5% for amplitudes above fifty percent of maximum amplitude, 2% for amplitudes between twenty five and fifty percent of maximum amplitude, 1% for amplitudes between ten and twenty five percent, and 0.5% below ten percent. The variable damping schedule for the random excitations was 5% for displacement amplitudes above .002 inches and 0.5% below .002 inches. A Newmark-Beta scheme was used to integrate the system (with an effective sample frequency of 500 samples per second) and develop traces that were five seconds long for impulse loading and twenty seconds long for random loading. For the random excitation cases, the damping for each step was set based on the displacement magnitude of the intermediate steps.

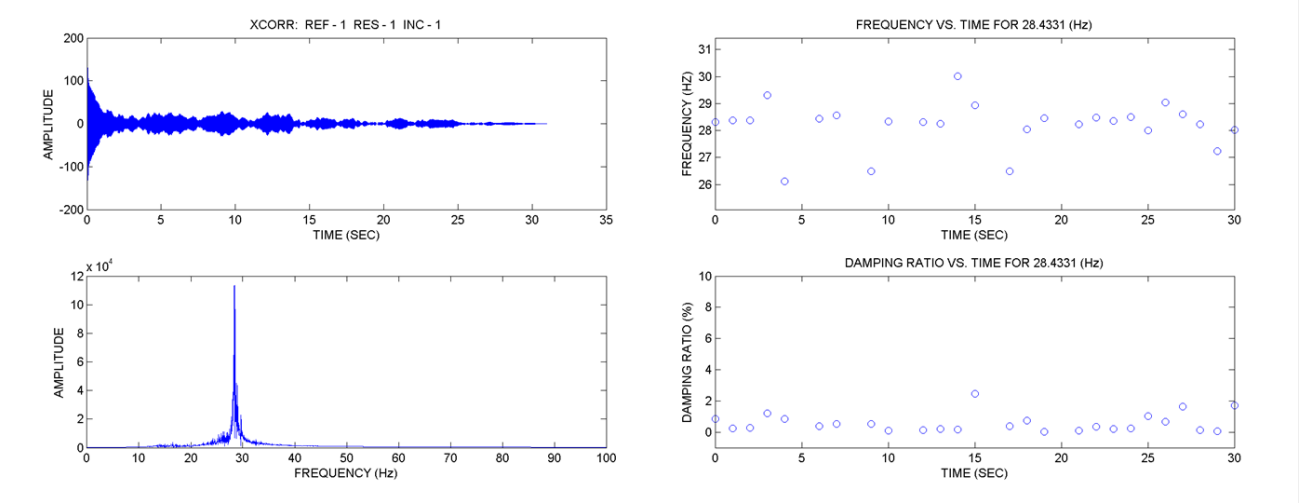

Figure 5. 30 Hz Variations for Sliding 1,000 Lag Window Analysis of Filtered Full-Length RR1 Autocorrelation

Table 1. Detailed Frequency and Damping for Early Lags of 30Hz Detailed Analysis of RR1 Data

Lags Used	Frequency #1 (Hz)	Damping #1 (%)	Frequency #2 (Hz)	Damping #2 (%)
1st 250	26.9	3.5	28.3	0.4
2nd 250	27.4	5.1	28.2	1.0
3rd 250	-	-	28.3	0.6
4th 250	-	-	28.3	1.1
1st 1000	-	-	28.2	0.8

The same analysis process was employed on this data as was used on the previous case studies (develop correlation functions and process with a time domain parameter estimation scheme). Figure 6 shows the impulse response (free decay) for the system with the variable damping (regions of the different damping levels are noted) as well as the associated correlation function. Table 2 shows the results of these impulse response data sets. It can be seen that the constant case with 0% added noise recovers the correct damping and frequency. Noise has a noticeable but not significant effect on the extracted values for this simple study. The variable damping data produced estimated modes at 10.1 Hz (6.2% damping) and 10.0 Hz (0.8% damping) when the correlation function was processed the same as the constant 0% noise case. The split modes with different damping values is expected but the over-compensation of the high damping levels is unexpected. Additionally, the variable damping correlation function was broken into 24 .2 second (100 sample) segments. The extracted damping for this part of the study was dependent on the segment analyzed (see Table 2). The early windows are strong in the higher damping and the later windows reproduce the lowest damping.

Figure 7 provides two functions. The left plot is the autocorrelation of a single time record under random loading with a constant damping. Notice the significant "beating" phenomena that is seen in the longer lags. This is a reproduction of the same effect seen in the first two case studies mentioned above. The right hand plot of Figure 7 shows an average of 20 of these correlation functions, each with a different random input. Notice that the "beating" phenomena is significantly reduced after averaging. In this study, averaging provided the most dramatic reduction in the "beating". Table 2 clearly shows the adverse effects of this beating on the damping estimates (1.4 to 3.0 for each of the 20 autocorrelation functions processed individually). This is not an unexpected finding but is critically important to understanding and potentially mitigating some difficulties in estimating damping from flight data. Most of the low frequency bands in flight data are not amenable to temporal averaging to reduce this inherent noise as the system is changing too rapidly. The alternatives are to use only the early part of the correlation functions, perform spatial averaging of several sensors, or utilizing force estimation procedures to attempt to reduce the random component of the responses.

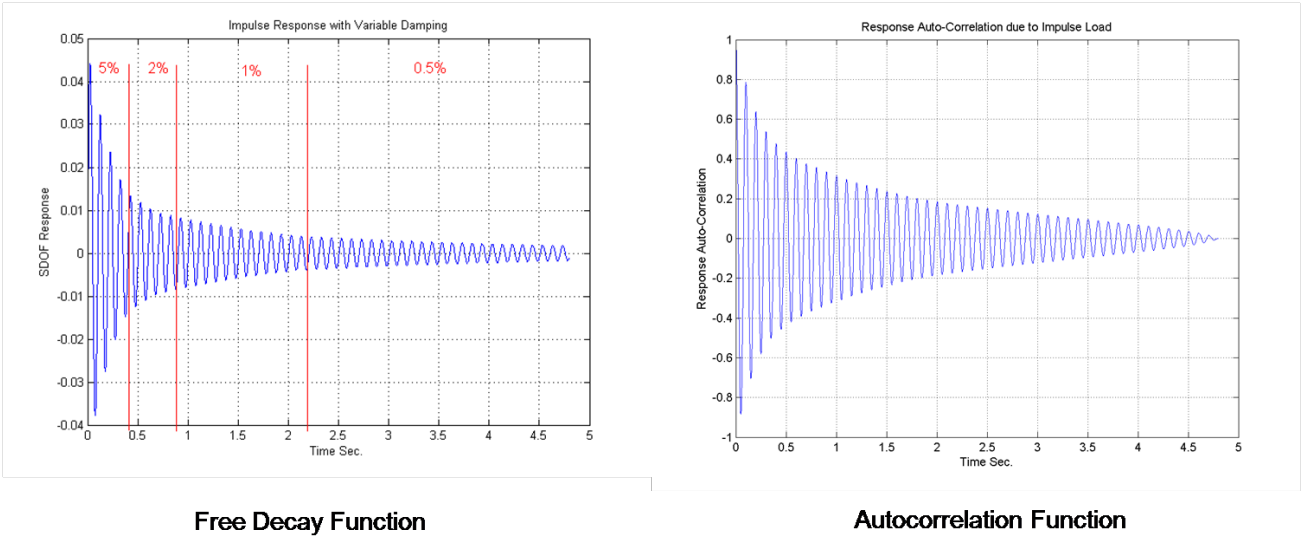

Figure 6. Impulse Response and Autocorrelation Functions for 10 Hz Case with 5.0% to .5% Variable Damping

Figure 8 shows the displacement response of the 10 Hz system with variable damping and a random input. Three different segments of the time history are denoted on the plot. The first exercise with the random data was to process these segments separately to understand how the damping might manifest itself. Auto-correlation functions associated with each segment are provided in the other plots of Figure 8. Table 2 shows the results of processing the correlation functions associated with these three segments. It can be seen that the modal frequency is extracted reasonably well but the damping values are different than expected (neither 5 Hz nor .5 Hz are found). This is an indication that the simulation of such a system is non-trivial and the approach used herein may be too simplistic. The hypothesis going into this study was that the early lags of the correlation function would be enhanced in the highly damped responses and the later lags would be enhanced in the lightly damped responses (as was seen with the impulse response loading). However, if this effect does exist it may not be manifested in this simplified approach.

The next numerical study performed was to assess the results of processing the complete autocorrelation function for the random loading/variable damping case. Table 2 shows the results from processing a correlation function and the results using an average of 20 correlation functions each with a different random input. The comparison seen in Figure 7 shows the effects of this averaging on the correlation functions. The comparative assessments are performed using a sequential series of .2 second windows taken from the single or average correlation functions. The results from the first three windows are very similar between the single and the average functions. Also, neither plot shows the expected 5% damping or the alternative 0.5% damping of the intended system. The resulting 1.3% is some combination of the two and is similar to the earlier results seen in processing different segments of the time record. The later windows, which utilize longer time lags, show much variation in damping as the numerical "beating" effect dominates the damping estimation. It is not

clear from the data provided in Table 2, but the average correlation function does produce consistent damping values for more windows than the single correlation function. However, once the windows of the average case enter the "beating" region, the damping values vary as much as those extracted from the single correlation function. The major conclusions are that it is advantageous to average correlation functions and focus on the early lags of the system. There are indications from the impulse data that the correlation function can maintain information on variable damping. However, this work has not yet shown that correlation functions of random excitation cases can retain that same information.

Table 2. Results of Numerical Study

Excitation Type	True Frequency (Hz)	True Damping (%)	Study Parameters	Estimated Frequency (Hz)	Estimated Damping (%)
Impulse	10.0	2.0	0% noise	10.0	2.0
Impulse	10.0	2.0	5% noise	10.0	2.1
Impulse	10.0	2.0	10% noise	10.0	2.3
Impulse	10.0	5.0 to 0.5	same parameters as constant case	10.1 and 10.0	6.2 and 0.8
Impulse	10.0	5.0 to 0.5	windows 1,2,3	10.0, 10.0, 10.0	4.7, 4.5, 1.75
Impulse	10.0	5.0 to 0.5	windows 4,5,6	10.0, 10.0, 10.0	0.9, 1.0, 1.0
Impulse	10.0	5.0 to 0.5	windows 7,8,9	10.0, 10.0, 10.0	1.0, 1.0, .9
Impulse	10.0	5.0 to 0.5	segments 10,11 to 24	10.0, 10.0, …, 10.0	0.6, 0.5, …, 0.5
Random	10.0	2.0	20 single traces	9.9 to 10.1	1.4 to 3.0
Random	10.0	2.0	20 trace average	10.0	2.0
Random	10.0	5.0 and 0.5	segment 1, 2, 3	10.0, 10.0, 9.9	6.0, 1.0, 1.7
Random	10.0	5.0 and 0.5	windows 1,2,3 (single trace)	10.0, 10.0, 10.0	1.3, 1.2, 1.2
Random	10.0	5.0 and 0.5	windows 4-23 (single trace)	9.8 – 10.0	0.3 – 2.1
Random	10.0	5.0 and 0.5	windows 1,2,3 (average trace)	10.0, 10.0, 10.0	1.3, 1.3, 1.3
Random	10.0	5.0 and 0.5	windows 4-23 (average trace)	10.0 – 10.0	-0.3 – 1.9

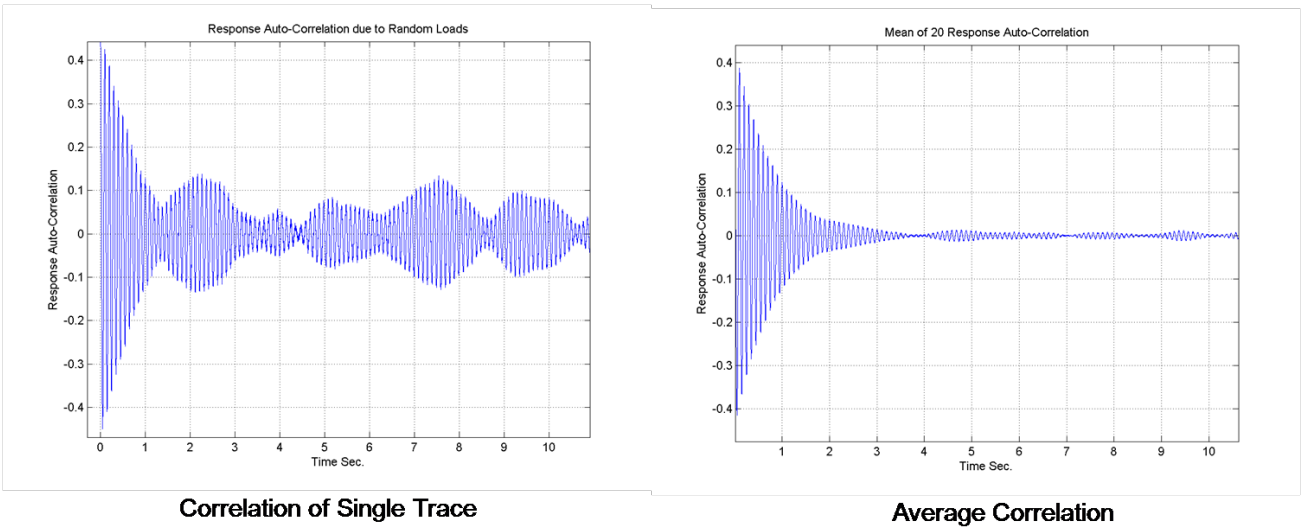

Figure 7. Autocorrelation Function of a Single Random Response and 20 Case Average (Constant Damping)

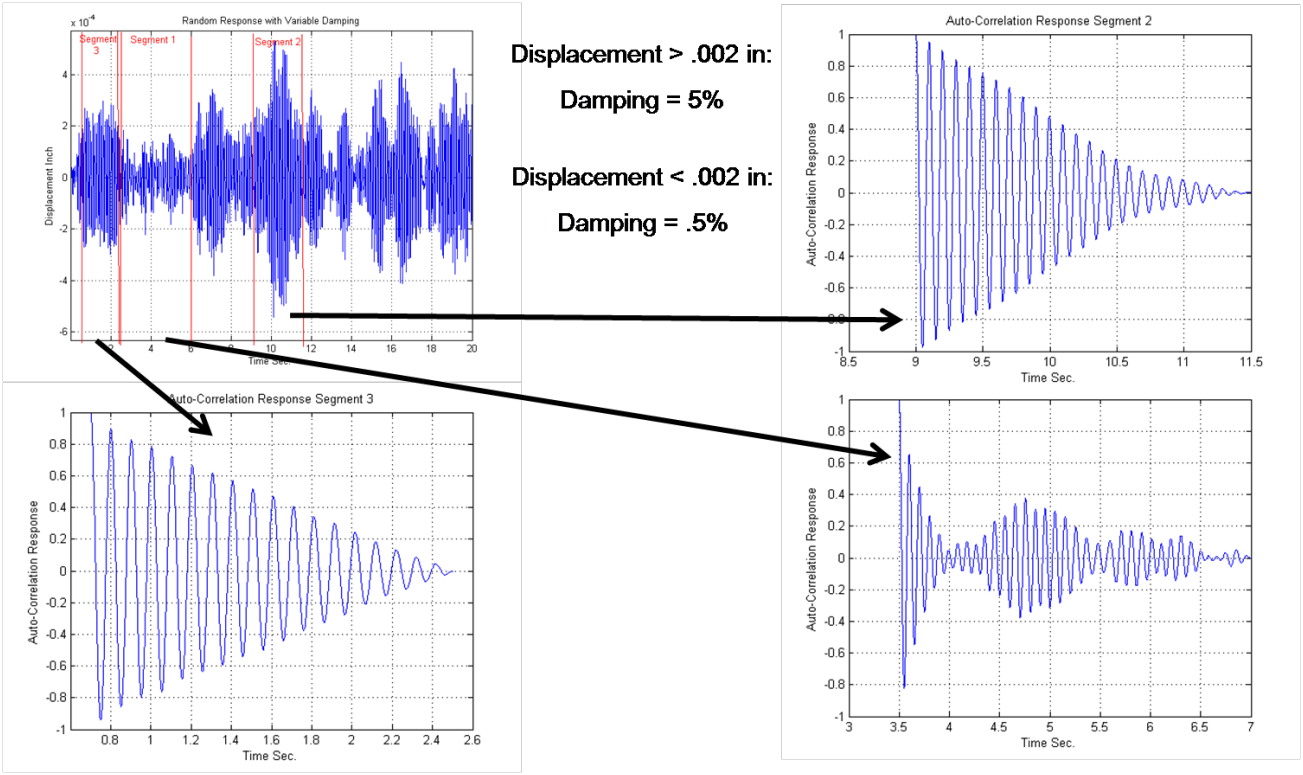

Figure 8. Displacement History and Acceleration Autocorrelation Function with Variable Damping

CASE STUDY 4 – ESCAPE SYSTEM FLIGHT DATA

The fourth case study is one of the most difficult applications of operation analysis that is available and the analysis efforts attempted to date have used insights gained from the case studies mentioned previously. The Pad Abort 1 test flight was a test flight of an escape system for a manned vehicle, which occurred in May 2010 at the U.S. Army's White Sands Missile Test Range near Las Cruces, NM. The test flight is characterized by very short and energetic excitations, rapidly depleting fuel, a wide range of excited frequencies, and high assumed flight damping estimates. Figure 9 shows the PA-1 vehicle in static and flight. The vehicle includes a Command Module (CM) test article with active flight control and data acquisition systems. The Launch Abort System (LAS) containing the motors for abort flight, steering control, and jettison is also an active part of the system.

The focus of the initial studies of this flight data have been on the very challenging early burn phase of flight, which is the first few seconds of flight with the highest excitation levels and the most rapidly changing system. A subset of 19 accelerometers covering both the CM and the LAS were used for these studies. Figure 10 provides example data from two of these sensors. These two sensors have been used as the "reference channel" in all the early burn analyses to date. Note that the time axis is given in terms of % of early burn and the frequency axis is provided in terms of % of sampling frequency to avoid any issues with current government-imposed data restrictions. This approach is intended to protect the sanctity of the data yet providing information that experts in the field can use to assess the results of this work.

Figure 11 provides the cross-correlation function between the two sensors shown in Figure 10 in the left hand plot. Also included in the plot is the sum of this cross-correlation function with of the other 18 correlation functions in the right hand plot (the sensor trace in the right hand plot in Figure 10 was used as the reference channel for all 19 correlations). This average of the 19 correlation functions is intended to implement the lessons learned in analytical studies shown previously. There are not enough time records (and the system is changing to fast) to average the data temporally, so this spatial averaging of data from a distributed set of sensors is used. Although neither of the functions shown in Figure 11

looks like the damped sinusoidal response expected, the sum of all correlation functions does show more distinct dynamic phenomena at the higher frequencies.

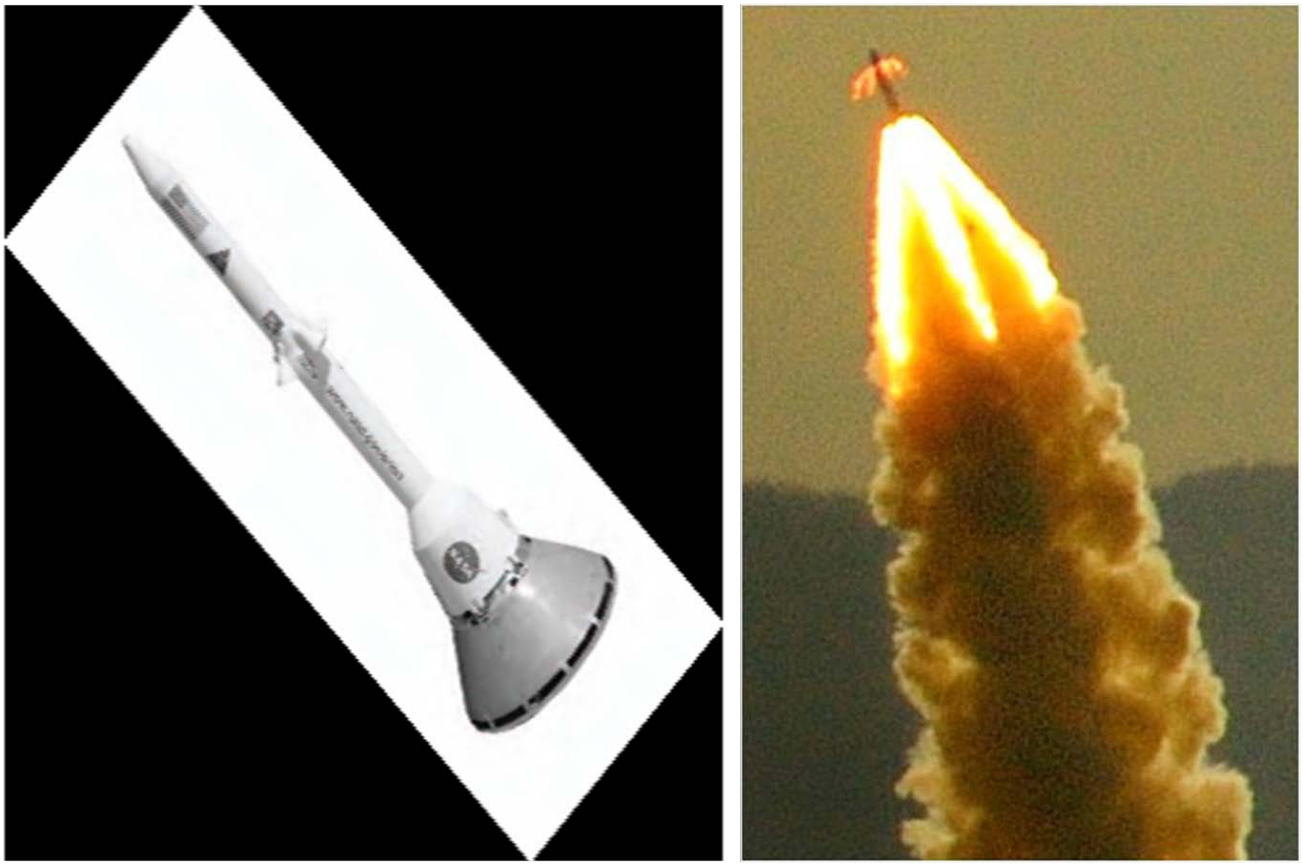

Figure 9. PA-1 Vehicle and Test Flight.

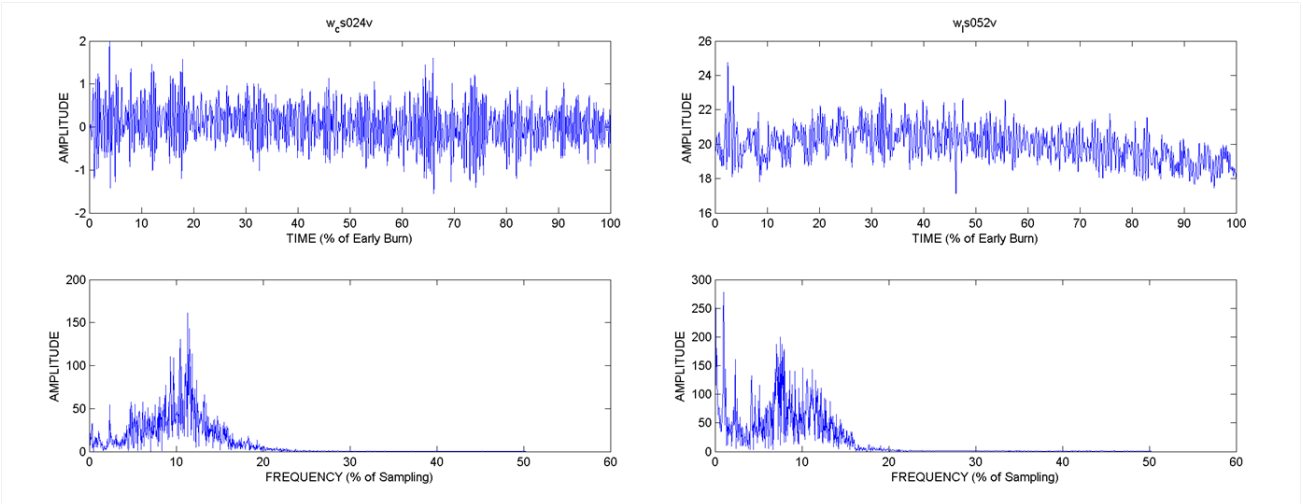

Figure 10. Two PA-1 Accelerometer Traces with Time and Frequency Domain Representations

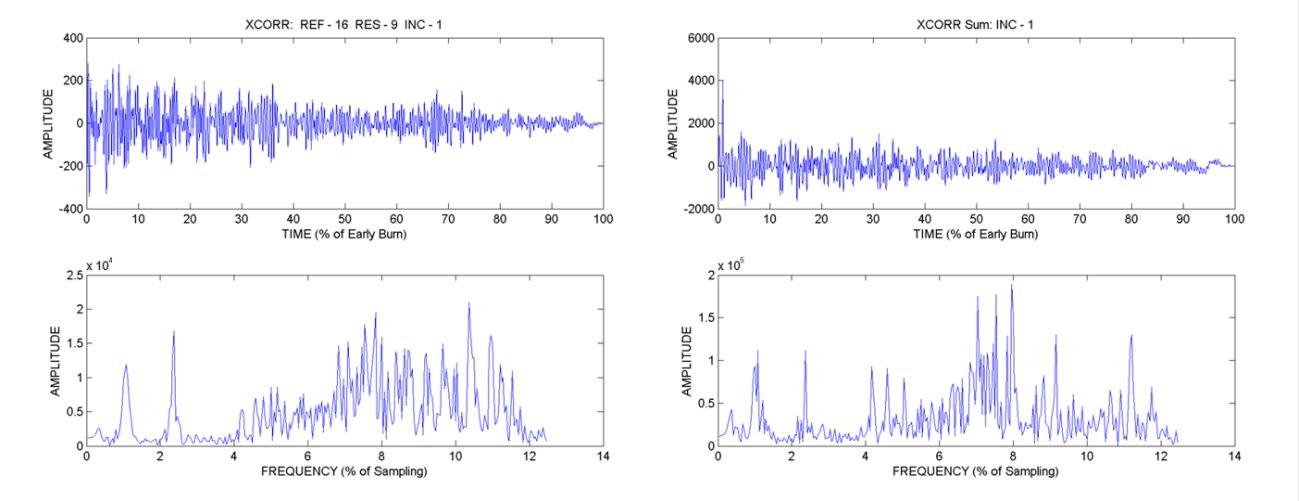

Figure 11. Cross-Correlation Function between Two PA-1 Responses with the Sum of 19 Correlations Functions

The most consistent analysis of the PA-1 data in this study has been focused on first three primary bending modes of the structure using 4th order Butterworth filters (used in a forward/reverse mode) around each assumed mode. The bandwidth of the filters is 1.2 % of the sampling frequency wide. A sliding window analysis is then used to assess the variability of the frequency and damping in each filtered dataset. Each sliding window is 21% of the total early burn time and is incremented by 1.3% of the early burn time to allow 60 separate analyses over the early burn flight time. Figure 12 shows an example of the results for the analysis around the first bending. The results for the sliding window analysis are provided in the left hand plot as well as the extracted results for a potential mode for the latter part of the burn (the right hand plot). In the sliding window analysis there are a significant number of noise modes, but more significantly are the consistent trends of the potential bending modes. Obtaining such consistent trends has been a primary focus of this flight data analyses to-date. The modal frequency has a reasonable and consistent trend for similar analyses. The damping has a trend but is not consistent (although similar to past flight damping estimates [10, 11]). The damping could be affected by the natural environment changes, control system forcing functions, or inconsistencies in the local fit. The next phase of this analysis would entail going to these specific windows between 63 and 71 and performing more detailed analyses. Regardless of additional work to understand this unusual trend, the results provided would suggest that typical values of 1% to 2% should be maintained for the damping in this mode for future flight analyses. Another finding is that the dynamic properties are changing too rapidly for the entire early burn to be used as a monolithic analysis.

Figure 13 contains the sliding window analysis results for a narrow band of frequencies around the second bending mode of the system in the left hand plot. There are several dynamic phenomena that show distinct trends. The mode that is likely one of the second bending modes is shown in the right hand plot. The frequency is showing a fairly consistent trend of increasing frequency as the fuel in the abort motor is quickly burned in this flight phase. The damping is showing quite a bit of variation throughout the flight (from 0.5% to 4%). Although this is similar to trends seen in previous flight data analyses [10, 11], the numerical study provided earlier suggests that the noise in the data could be significantly affecting damping. However, the assessment of the data if taken at face value is that typical damping values of 1% to 2% should be maintained for this frequency range until additional analyses can be performed.

Figure 14 provides the sliding window analyses for the region around the third bending mode. As expected, there are an increasing number of dynamic phenomena as the frequency band increases. There are also more consistent trends and fewer noise modes in this analysis than at the lower modes. This is potentially due to the fact that there is more apparent excitation in the frequency bands (see Figures 10 and 11) and there are more cycles of the damped sinusoids in each window of correlation data analyzed. However the frequency and damping trends are similar to what was seen in the earlier frequency bands. The increasing modal density suggests that it would be useful to perform shape fitting to the correlation functions of the individual sensors to extract information help in determining the true nature of the dynamic phenomena captured in these results.

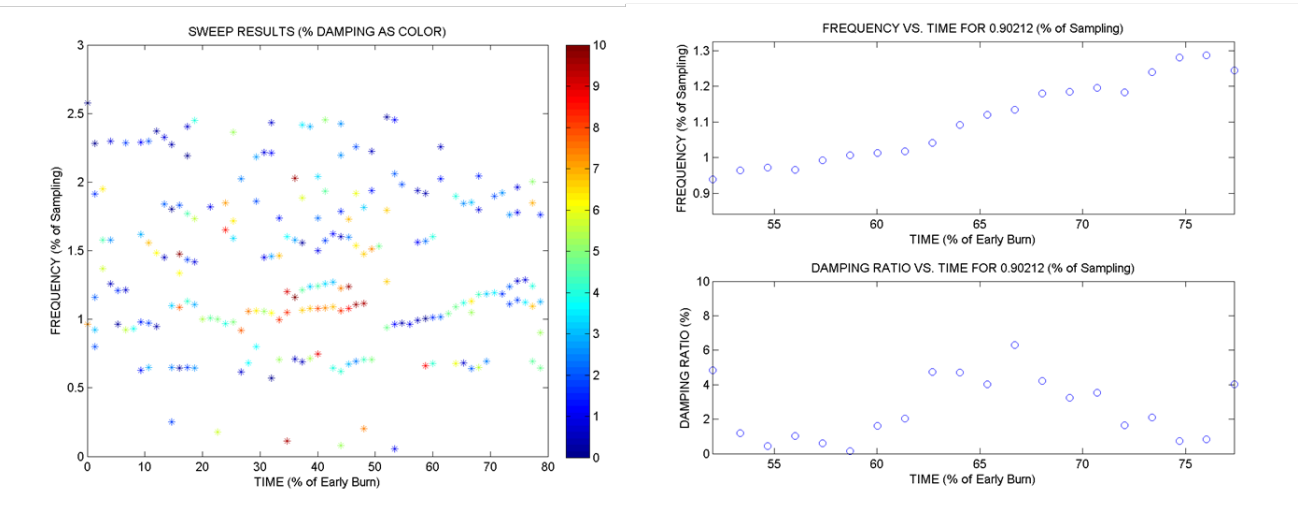

Figure 12. PA-1 Early Burn Results for Sliding Window Analysis around the First Bending Mode

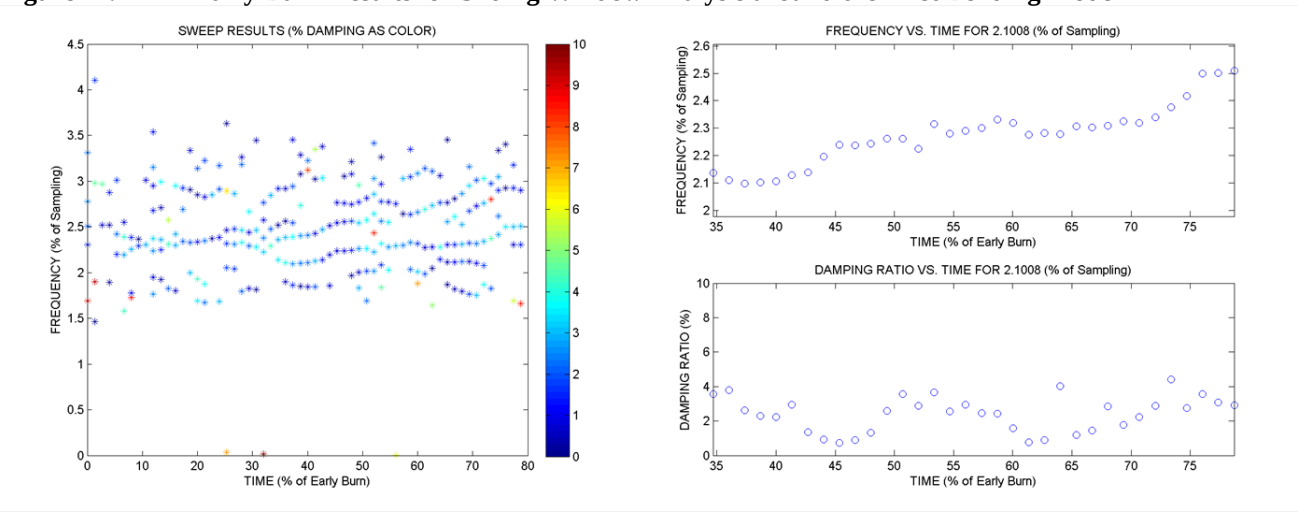

Figure 13. PA-1 Early Burn Results for Sliding Window Analysis around the Second Bending Mode

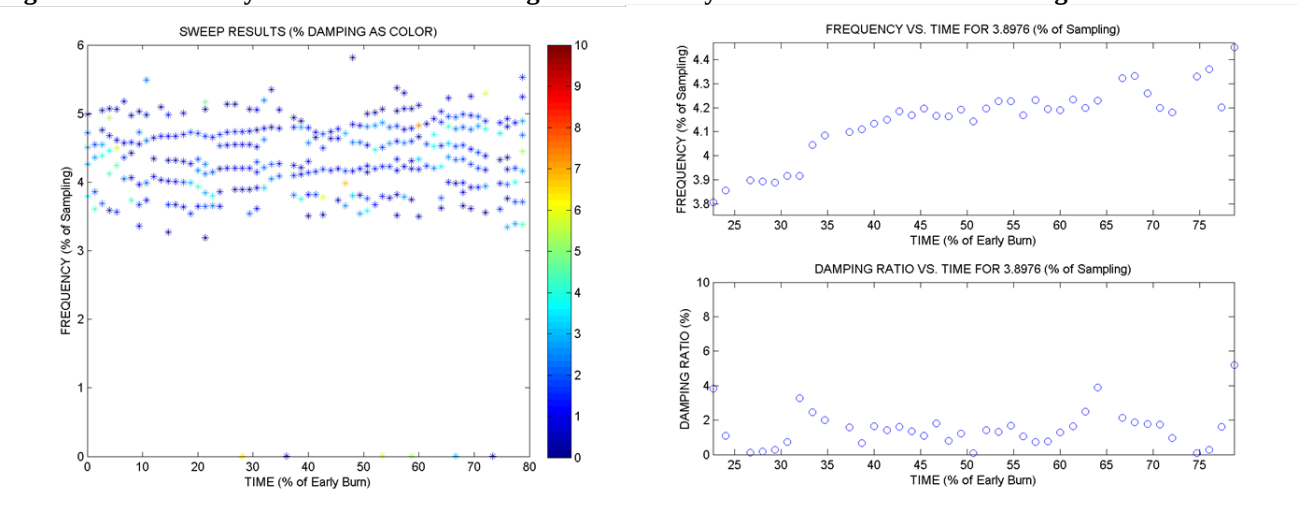

Figure 14. PA-1 Early Burn Results for Sliding Window Analysis around the Third Bending Mode

CONCLUSIONS

Although the information reported herein is a work in progress, there are several preliminary conclusions that could be drawn from the four case studies mentioned herein. First the most prevalent feature of the analyses performed herein is the "beating" phenomena seen in the random excitation data that is typically reduced by averaging in non-flight data sets. There were three tools used to help clear up the analyses issues reported in this paper (including the "beating" effect): spatially averaging several sensors correlation functions, using the earliest lags in the correlation functions, and applying fairly tight bandpass filters to the data. Also, additional analysis of local time segments is needed to find the true cause for the variations in damping seen in the extracted modes. There are several additional suggestions for forward work that have been suggested: continue to understand the complexities of simulating random excitation/variable damping systems; implement, apply, and assess more advanced operational analysis tools; perform shape estimations as the next step in such analyses; and apply force reconstruction techniques to reduce some of the detrimental noise/forcing function effects. In addition, a widely distributed set of time-synchronized flight sensors should be developed, flown, and used for analyses to expand the state-of-the-art.

REFERENCES

1. Brinker R and Kirkegaard P (2010) Special issue on operational modal analysis. Editorial in Mechanical Systems and Signal Processing, Vol. 24, No. 5, pp. 1209-1212.
2. Carne T and James G (2010) The inception of OMA in the development of modal testing technology for wind turbines. Mechanical Systems and Signal Processing, Vol. 24, No. 5, pp. 1213-1226.
3. James G, Carne T, and Lauffer J (1995) The Natural Excitation Technique (NExT) for modal parameter extraction from operating structures. SEM International Journal of Analytical and Experimental Modal Analysis, Vol. 10, No. 4.
4. Brownjohn J and Carden P (2007) Reliability of frequency and damping estimates from free vibration response. Proceedings of the 2nd International Operational Modal Analysis Conference, pp 23-30.
5. Zhang L, Wang T, and Tamura Y (2010) A Frequency-Spatial Domain Decomposition (FSDD) method for operational modal analysis. Mechanical Systems and Signal Processing, Vol. 24, No. 5, pp. 1227-1239.
6. Magalhães F, Cunha A, Caetano E, and Brinker R (2010) Damping estimation using free decays and ambient vibration tests. Mechanical Systems and Signal Processing, Vol. 24, No. 5, pp. 1274-1290.
7. Agneni A, Crema L B, and Coppotelli G (2010) Output-only analysis of structures with closely spaced poles. Mechanical Systems and Signal Processing, Vol. 24, No. 5, pp. 1241-1249.
8. Bjerg I, Hansen S, Brinker R, and Aenlle M L (2007) Load estimation by frequency domain decomposition. Proceedings of the 2nd International Operational Modal Analysis Conference, pp 669-676.
9. James G, Carne T, and Wilson B (2007) Reconstruction of the Space Shuttle roll-out forcing function. Proceedings of the 25th International Modal Analysis Conference.
10. James G, Carne T, and Edmunds R (1994) STARS missile – modal analysis of first flight data using the Natural Excitation Technique (NExT). Proceedings of the 12th International Modal Analysis Conference.
11. James G, Carne T, and Marek E (1994) In-situ modal analysis of STARS missile flight data and comparison to pre-flight predictions from test-reconciled models. Proceedings of the 15th Institute of Environmental Sciences Aerospace Testing Seminar.
12. Kim H, VanHorn D, and Doiron H (1994) Free-decay time-domain modal identification for large space structures. Journal of Guidance, Control, and Dynamics, Vol. 17, No. 3, pp. 513-519.
13. James G (2003) Modal parameter estimation from Space Shuttle flight data. Proceedings of the 21st International Modal Analysis Conference.
14. Le Gallo V, Goursat M, and Gonidou L (2007) Damping characterization and flight identification. Proceedings of the 25th International Modal Analysis Conference.
15. Goursat M, Döhler M, Mevel L, and Andersen P (2010) Crystal Clear SSI for Operational Modal Analysis of Aerospace Vehicles. Proceedings of the 28th International Modal Analysis Conference.
16. Fransen S, Rixen D, Henricksen T, and Bonnet M (2010) On the operational modal analysis of solid rocket motors. Proceedings of the 28th International Modal Analysis Conference
17. Bartkowicz T and James G (2011) Ares 1-X in-flight modal identification. Submitted to the American Institute of Aeronautics and Astronautics Structures, Structural Dynamics, and Materials Conference.
18. Pappa R, James G, and Zimmerman D (1999) Application of autonomous modal identification of the Space Shuttle tail rudder. AIAA Journal of Spacecraft and Rockets, Vol. 35, No. 2, pp. 163-169.
19. James G, Chhipwadia K, and Zimmerman, D (1999) Application of autonomous modal identification to traditional and ambient data sets. Proceedings of the 17th International Modal Analysis Conference.
20. Pappa R, Elliott K, and Schenk A (1993) Consistent mode indicator for the eigensystem realization algorithm. Journal of Guidance, Dynamics, and Control, vol. 16, no. 5, pp. 852-858.